Soft proton exchanged channel waveguides in congruent lithium tantalate for frequency doubling

Alessandro C. Busacca,[1*] Salvatore Stivala,[1] Luciano Curcio,[1] Paolo Minzioni,[2] Giovanni Nava,[2] Ilaria Cristiani,[2] and Gaetano Assanto[3]

[1]DIEET, University of Palermo, Viale delle Scienze, Bldg. no. 9, 90128 Palermo, Italy
[2]CNISM & Electronics Dept., University of Pavia, Via Ferrata 1, 27100 Pavia, Italy
[3]Nonlinear Optics and OptoElectronics Lab, University "Roma Tre", Via della Vasca Navale 84, 00146 Rome, Italy
[*]busacca@unipa.it

Abstract: We report on stable optical waveguides fabricated by soft-proton exchange in periodically-poled congruent lithium tantalate in the α-phase. The channel waveguides are characterized in the telecom wavelength range in terms of both linear properties and frequency doubling. The measurements yield a nonlinear coefficient of about 9.5pm/V, demonstrating that the nonlinear optical properties of lithium tantalate are left nearly unaltered by the process.

OCIS codes: (190.4390) Nonlinear optics, integrated optics; (130.3130); Integrated optics materials; (230.7370) Waveguides; (230.4320) Nonlinear optical devices.

References and links

1. R. DeSalvo, D. J. Hagan, M. Sheik-Bahae, G. Stegeman, E. W. Van Stryland, and H. Vanherzeele, "Self-focusing and self-defocusing by cascaded second-order effects in KTP," Opt. Lett. **17**(1), 28–30 (1992).
2. G. Assanto, G. I. Stegeman, M. Sheik-Bahae, and E. VanStryland, "All Optical Switching Devices Based on Large Nonlinear Phase Shifts from Second Harmonic Generation," Appl. Phys. Lett. **62**(12), 1323–1325 (1993).
3. G. Assanto, Z. Wang, D. J. Hagan, and E. VanStryland, "All Optical Modulation via Nonlinear Cascading in Type II Second Harmonic Generation," Appl. Phys. Lett. **67** (15), 2120–2122 (1995).
4. G. Assanto, G. I. Stegeman, and R. Schiek, "Thin film devices for all-optical switching and processing via quadratic nonlinearities," Thin Solid Films **331**(1-2), 291–297 (1998).
5. A. Buryak, P. Di Trapani, D. Skryabin, and S. Trillo, "Optical solitons due to quadratic nonlinearities: from basic physics to futuristic applications," Phys. Rep. **370**(2), 63–235 (2002).
6. K. Gallo, G. Assanto, and G. I. Stegeman, "Efficient Wavelength Shifting Over the Erbium Amplifier Bandwidth Via Cascaded Second Order Processes in Lithium Niobate Waveguides," Appl. Phys. Lett. **71**(8), 1020–1022 (1997).
7. I. Cristiani, M. Rini, A. Rampulla, G. P. Banfi, and V. Degiorgio, "Wavelength conversion of an infrared signal through cascaded second-order nonlinearity in a lithium-niobate channel waveguide," J. Nonlinear Opt. Phys. Mater. **9**, 11–20 (2000).
8. M. H. Chou, K. R. Parameswaran, M. M. Fejer, and I. Brener, "Multiple-channel wavelength conversion by use of engineered quasi-phase-matching structures in LiNbO/sub 3/ waveguides," Opt. Lett. **24**(16), 1157–1159 (1999).
9. Y. L. Lee, H. Suche, Y. H. Min, J. H. Lee, W. Grundkotter, V. Quiring, and W. Sohler, "Wavelength- and time-selective all-optical channel dropping in periodically poled Ti : LiNbO/sub 3/ channel waveguides," IEEE Photon. Technol. Lett. **15**(7), 978–980 (2003).
10. A. Mecozzi, C. B. Clausen, and M. Shtaif, "System impact of intra-channel nonlinear effects in highly dispersed optical pulse transmission," IEEE Photon. Technol. Lett. **12**(12), 1633–1635 (2000).
11. P. V. Mamyshev, and N. A. Mamysheva, "Pulse-overlapped dispersion-managed data transmission and intrachannel four-wave mixing," Opt. Lett. **24**(21), 1454–1456 (1999).
12. M. M. Fejer, G. A. Magel, D. H. Jundt, and R. L. Byer, "Quasi-phase-matched second harmonic generation: tuning and tolerances," IEEE J. Quantum Electron. **28**(11), 2631–2654 (1992).
13. D. A. Akimov, M. Schmitt, R. Maksimenka, K. V. Dukel'skii, Y. N. Kondrat'ev, A. V. Khokhlov, V. S. Shevandin, W. Kiefer, and A. M. Zheltikov, "Supercontinuum generation in a multiple-submicron-core microstructure fiber: toward limiting waveguide enhancement of nonlinear-optical processes," Appl. Phys. B **77**(2-3), 299–305 (2003).
14. G. I. Stegeman, and G. Assanto, "Nonlinear Integrated Optical Devices," Chap. 11, pp. 381–418 in *Integrated Optical Circuits and Components: Design and Application*, ed. E. J. Murphy, (M. Dekker, New York, 1999).

15. W. Sohler, H. Hu, R. Ricken, V. Quiring, C. Vannahme, H. Herrmann, D. Büchter, S. Reza, W. Grundkötter, S. Orlov, H. Suche, R. Nouroozi, and Y. Min, "Integrated Optical Devices in Lithium Niobate," Opt. Photon. News **19**(1), 24–31 (2008).
16. Y. Furukawa, K. Kitamura, S. Takekawa, K. Niwa, and H. Hatano, "Stoichiometric Mg:LiNbO/sub 3/ as an effective material for nonlinear optics," Opt. Lett. **23**(24), 1892–1894 (1998).
17. Y. Kondo, and Y. Fujii, "Temperature Dependence of the Photorefractive Effect in Proton-Exchanged Optical Waveguides Formed on Lithium Tantalate Crystals," Jpn. J. Appl. Phys. **34**(Part 2, No. 3B), 365–367 (1995).
18. M. Marangoni, M. Lobino, R. Ramponi, E. Cianci, and V. Foglietti, "High quality buried waveguides in stoichiometric LiTaO/sub 3/ for nonlinear frequency conversion," Opt. Express **14**(1), 248–253 (2006), http://www.opticsinfobase.org/oe/abstract.cfm?uri=oe-14-1-248.
19. V. Rastogi, P. Baldi, I. Aboud, P. Aschieri, M. P. De Micheli, D. B. Ostrowsky, and J. P. Meyn, "Effect of proton exchange on periodically poled ferroelectric domains in lithium tantalate," Opt. Mater. **15**(1), 27–32 (2000).
20. P. Baldi, S. Nouh, K. E. Hadi, M. Micheli, D. B. Ostrowsky, D. Delacourt, and M. Papuchon, "Quasi-phase-matched parametric fluorescence in room-temperature lithium tantalate waveguides," Opt. Lett. **20**(13), 1471–1473 (1995).
21. K. El Hadi, P. Baldi, S. Nouh, M. P. De Micheli, A. Leycuras, V. A. Fedorov, and Y. N. Korkishko, "Control of proton exchange for LiTaO3 waveguides and the crystal structure of H/sub x/Li/sub (1-x)/TaO/sub 3/," Opt. Lett. **20**(16), 1698–1700 (1995).
22. A. C. Busacca, E. D'Asaro, S. Riva Sanseverino, and G. Assanto, "Stable Proton Exchanged Waveguides in Lithium Tantalate," IEEE Photon. Technol. Lett. **20**(24), 2126–2128 (2008).
23. A. Parisi, A. C. Cino, A. C. Busacca, and S. Riva-Sanseverino, "Nonstoichiometric silica mask for fabricating reverse proton-exchanged waveguides in lithium niobate crystals," Appl. Opt. **43**(4), 940–943 (2004).
24. M. de Micheli, D. B. Ostrowsky, J. P. Barety, C. Canali, A. Carnera, G. Mazzi, and M. Papuchon, "Crystalline and optical quality of proton exchanged waveguides," J. Lightwave Technol. **4**(7), 743–745 (1986).
25. I. Cristiani, C. Liberale, V. Degiorgio, G. Tartarini, and P. Bassi, "Nonlinear characterization and modeling of periodically poled lithium niobate waveguides for 1.5-μm-band cascaded wavelength conversion," Opt. Commun. **187**(1-3), 263–270 (2001).
26. S. Stivala, A. Pasquazi, L. Colace, G. Assanto, A. C. Busacca, M. Cherchi, S. Riva-Sanseverino, A. C. Cino, and A. Parisi, "Guided-wave frequency doubling in surface periodically poled lithium niobate: competing effects," J. Opt. Soc. Am. B **24**(7), 1564–1570 (2007).
27. A. C. Busacca, E. D'Asaro, A. Pasquazi, S. Stivala, and G. Assanto, "Ultraviolet generation in periodically poled lithium tantalate waveguides," Appl. Phys. Lett. **93**(12), 121117 (2008).

1. Introduction

Optical frequency conversion via parametric mixing in second-order nonlinear crystals is a key technology for wavelength generation and signal processing at high bit-rates. Besides the various applications via quadratic cascading [1–5], parametric effects have been proposed and implemented towards channel dropping/shifting, dispersion compensation and the suppression of nonlinear interactions experienced by optical pulses [6–11].

Nowadays, mature Quasi-Phase-Matching (QPM) techniques [12] in conjunction with low-loss waveguides have increased by orders of magnitude the efficiency of quadratic interactions, allowing $\chi^{(2)}$-based integrated devices to compete even with record high $\chi^{(3)}$ nonlinearities achieved e. g. through fiber microstructuring and glass engineering [13]. High quality QPM gratings are often implemented in waveguides realized in ferroelectric crystals such as Lithium Niobate (LN) and Lithium Tantalate (LT), as dielectric confinement can enhance nonlinear effects as compared to free propagation in bulk [14]. Nowadays, QPM periodically poled lithium niobate (PPLN) can be prepared with propagation lengths up to several inches, thereby optimizing parametric conversion and wave mixing effects with precise tuning of the phase matching condition usually achieved by controlling the operating temperature [15]. A concern about wavelength conversion in PPLN waveguides is the photorefractive effect (PRE), since LN crystals are vulnerable to high-power light irradiation [16]. To suppress or drastically reduce the PRE, high-efficiency devices based on LN for signal processing in the C band need be operated at relatively high temperature, generally above 100°C, thus making difficult their practical utilization in actual links.

At variance with PPLN, optical waveguides in PP Lithium Tantalate (PPLT) offer superior resistance to the PRE [17] and provide reasonable conversion efficiency, as demonstrated with stoichiometric LT substrates [18]. Among the available processes for waveguide fabrication in LT, the most successful are those based on proton exchange (PE), whose compatibility with LT poling was demonstrated in Ref [19–21]. Since low proton concentration affects only slightly the crystal stoichiometry, stable α-phase channel waveguides in congruent PPLT

(cPPLT) can be realized by PE [22]. Noteworthy, α-phase waveguides preserve LT nonlinear properties and show a better long-term stability when compared to samples prepared with other fabrication techniques, or different proton-exchange conditions [22]. To date, however, guided-wave devices operating at telecom wavelengths were never demonstrated in electric field PP congruent LT. In this paper we report the first fabrication and characterization of integrated frequency doublers in cPPLT, operating in the C-band (1525-1565nm) of fiber communication systems.

2. Waveguide fabrication and linear characterization

The samples were prepared following two main technological steps: (i) realization of QPM gratings by electric-field assisted periodic poling of LT z-cut substrates, (ii) fabrication of channel waveguides by soft proton exchange. A commercial (Yamaju Ceramics) congruent LT wafer (z-cut, 500μm thick) was diced into rectangular samples (16 mm × 30 mm) prior to spin-coating with a 2 μm thick photoresist (Shipley S1813) film on the −z facet. Standard lithography was employed to realize a 2.25 cm long grating with period $\Lambda = 20.8$μm along x. An overnight soft-baking (90°C) and a 3h long 130°C baking were necessary to ensure both a good adhesion of the photoresist to the substrate and an adequate electric insulation. Higher temperature would eventually result in photoresist melting and/or carbonization. The temperature was gradually raised in order to avoid the pyroelectric effect, the formation of poling dots and the insurgence of mechanical stress in the crystal. The sample was placed between gel electrolyte layers to provide low-resistance electric contact. In order to exceed the LT coercive field and obtain a controlled periodic inversion of the ferroelectric domains, we used a voltage amplified waveform generator to apply 1.3 kV pulses over a 10 kV bias for appropriate time intervals. With this approach, the inverted domains enucleated from the −z facet in the region under the electrodes and extended towards the + z facet.

LT channel waveguides were fabricated on the −z facet of the crystal using a lithographically patterned 70nm-thick SiO_2 mask [23]. We prepared a set of 2.4cm-long channel waveguides of widths ranging from 8 to 13μm using the "sealed ampoule" PE technique [24]. A melted mixture of Benzoic Acid and 3.6% Lithium Benzoate preserved the nonlinear optical properties and domain orientation of the crystal, realizing "soft PE" waveguides in the α-phase. Proton exchange for 144 hours at ≈300°C yielded single mode waveguides at telecom wavelengths. The TM_0 corresponding effective index was measured at 1.55μm in the planar waveguide on the + z face of the same sample using dark m-line spectroscopy and the prism coupling technique. The overall effective index increase with respect to the extraordinary refractive index of the substrate for the fundamental transverse-magnetic (TM) mode was estimated around 2×10^{-3}. Finally, the chip end-facets were polished to optical grade to allow efficient in and out coupling to radiation modes.

The characterization was carried out at room-temperature with a wavelength tunable external-cavity laser (ECL) linearly polarized and butt-coupled to the waveguides in order to excite TM modes; we used micro-positioners and standard single-mode fibers with an effective area $A_{eff} = 80$μm^2 and propagation losses $\alpha = 0.2$ dB km^{-1} at 1550nm. The output light was collected via either a microscope objective or fiber end-fire coupling, depending on the measured quantity. The overall (fiber to fiber) insertion losses in the waveguide amounted to 7dB. From our measurements the coupling loss at each waveguide facet resulted equal to 1.2dB, and hence we estimated the propagation losses in about 2 dB cm^{-1}

To evaluate the waveguide modal area in the range 1525-1565nm, we analyzed the magnified image of the output mode, created by using microscope objective, with a calibrated Vidicon camera. Figure 1(a) displays a typical image of the optical TM_{00} mode in a channel of nominal width 13μm, with Fig. 1(b) and Fig. 1(c) showing horizontal and vertical transverse profiles, respectively.
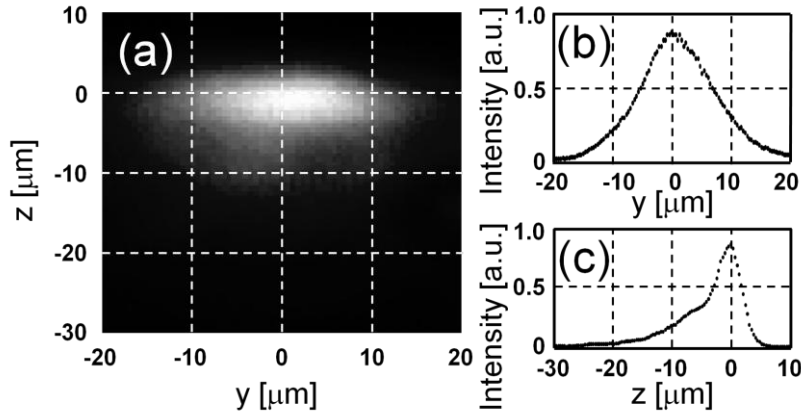
Fig. 1. (a) Near infrared mode measured at the output of the 13μm-wide channel waveguide at 1550nm; (b) and (c) graph horizontal and vertical profiles, respectively. Here the LT-air surface corresponds to the zero of the coordinate z in (a) and (c).

The TM_{00} effective area was $\approx$455 μm^2 at $1/e^2$ ($\approx$110 μm^2 at 1/2) with respect to the peak intensity distribution. As visible in Fig. 2 and expected, the fundamental TM mode was better confined in wider waveguides because, due to the low index increase, in narrow waveguides a significant part of the optical power propagated into the substrate.
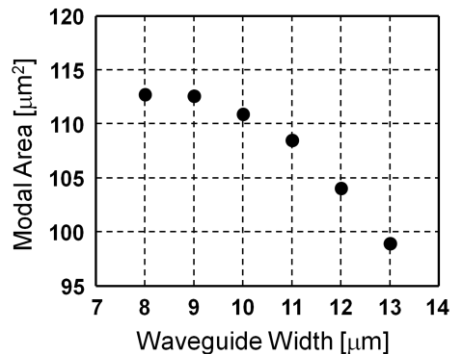

Fig. 2. TM_{00} modal area (at 1/2 peak) measured at 1550nm versus nominal waveguide width.

3. Nonlinear characterization

The nonlinear properties of the samples were evaluated in terms of Second Harmonic Generation (SH-G). Owing to the higher equivalent frequency (or thickness) of the waveguide at SH, several TM modes of SH were supported by each channel. By tuning the fundamental frequency (FF) wavelength of the ECL we were able to achieve phase-matching on three distinct resonances: phase matching at $\approx$1567nm corresponded to the interaction between the FF TM_{00} pump and the TM_{00} mode of the SH; phase matching at $\approx$1555nm and $\approx$1552nm stemmed from the interactions between the FF TM_{00} and SH TM_{20} and TM_{01} modes, respectively. As expected, no SHG resonance was observed corresponding to phase matching with the SH TM_{10} mode [25].

In line with numerical simulation of the corresponding modal profiles for FF and SH TM modes, the highest conversion efficiency was obtained by phase-matching the FF TM_{00} pump and the SH TM_{01} mode. Owing to the different degrees of confinement and vertical (i.e. along z) offsets of FF and SH modes (see Fig. 3), the TM_{01} mode at SH yielded the largest overlap integral with the fundamental frequency pump TM_{00} [26,27], resulting in $\approx$0.0408μm^{-1}.
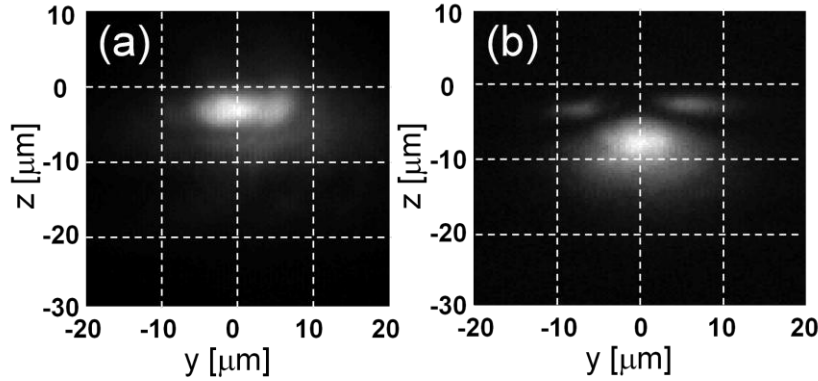
Fig. 3. SH Modal profiles measured at the respective resonances and taken at the output of a 13µm-wide channel: (a) fundamental mode TM_{00}; (b) TM_{01} mode.

From the measurement of SHG conversion efficiency versus FF wavelength, presented in Fig. 4(a), we evaluated the effective length of the nonlinear interaction to be ≈ 2.25 cm [12], such a value being very close to the actual extension of the QPM grating. This result can be ascribed to the weak confinement of the pump mode, with light experiencing an effective refractive index very close to that of the substrate. Nevertheless, it gives also an indication of the good uniformity of the periodically poled grating and of the waveguide profile. The latter parameter can be very critical as a constant waveguide cross section is crucial to maintain phase-matching over the whole propagation length [25]. From the averaged experimental data shown in Fig. 4(b) and collected in the case of the most efficient QPM interaction, i.e. the SH TM_{01} with the FF TM_{00}, we evaluated a waveguide SHG efficiency of $0.07\% W^{-1}cm^{-2}$.
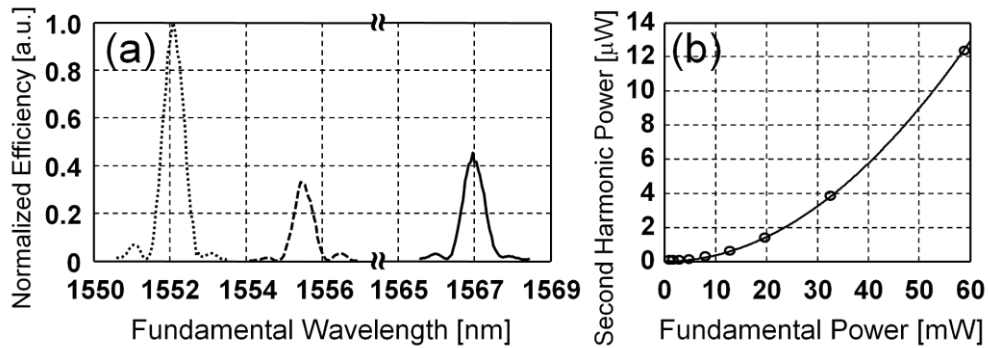

Fig. 4. (a) Measured normalized SHG conversion efficiency versus FF wavelength. The three peaks correspond to the FF interaction with the TM_{00} (solid line), TM_{20} (dashed line) and TM_{01} (dotted line) SH modes. (b) SH power versus FF excitation with a TM_{00} mode: data (symbols) and parabolic fit (solid line).

Noteworthy, our measurements indicate that the PM condition for the SH TM_{01} mode is not critical, i.e. the PM wavelength is weakly dependent on the waveguide size. This eases the requirements on uniformity and helps obtaining efficient nonlinear conversion in the regions with the quasi-phase-matching grating was fabricated (Fig. 5).
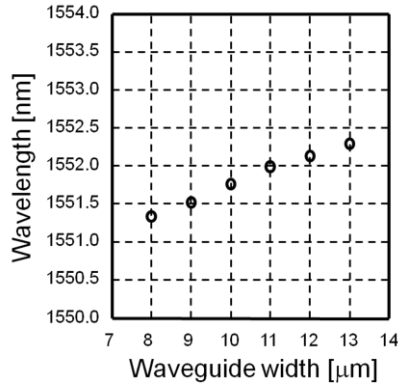
Fig. 5. PM wavelength shift versus waveguide width.

4. Conclusions

In conclusion, we reported on the first realization of α-phase low-loss channel waveguides in electric field periodically poled LT for signal transmission and quasi phase matched second harmonic generation from telecom wavelengths. The soft proton exchanged waveguides confine light better in wider channels and provide quasi phase matching of the TM_{00} mode at the fundamental frequency with higher-order second-harmonic TM modes.

Acknowledgements